



The 7th World Congress on Particle Technology (WCPT7)

## CFD Simulation of a Counter-Current Spray Drying Tower with Stochastic Treatment of Particle-Wall Collision

Muzammil Ali<sup>a</sup>, Tariq Mahmud<sup>a,\*</sup>, Peter John Heggs<sup>a</sup>, Mojtaba Ghadiri<sup>a</sup>, Andrew Bayly<sup>a</sup>, Hossein Ahmadian<sup>b</sup> and Luis Martin de Juan<sup>b</sup>

<sup>a</sup>*Institute of Particle Science and Engineering, School of Process, Environmental and Materials Engineering, University of Leeds, LS2 9JT, UK*

<sup>b</sup>*Procter and Gamble, Whitley Road, Longbenton Newcastle Upon Tyne, NE12 9TS, UK*

### Abstract

In this study, a steady state, three-dimensional, multiphase CFD modeling of a pilot-plant counter-current spray drying tower is carried out to study the drying of detergent slurry and to predict spray-dried detergent powder characteristics. The coupling between the two phases is achieved using the Eulerian-Lagrangian approach. The continuous phase turbulence is modeled using the Reynolds stress transport model. The droplet drying kinetics is studied using a semi-empirical droplet/particle drying model. Emphasis is given on the modeling of particle-wall interaction by considering only the rebound effect and specifying the coefficient of restitution as a function of impact angle with wall surface roughness taken into account using a stochastic approach, as well as a function of moisture content. This influences the post-wall collision trajectories of particles, residence time distribution and the overall exchange of heat and mass transfer. The model predictions agree well with the measured outlet values of powder average temperature, moisture content and exhaust air temperature considering the complexity of the process and the measurements accuracy.

© 2015 Published by Elsevier Ltd. This is an open access article under the CC BY-NC-ND license (<http://creativecommons.org/licenses/by-nc-nd/4.0/>).

Selection and peer-review under responsibility of Chinese Society of Particuology, Institute of Process Engineering, Chinese Academy of Sciences (CAS)

*Keywords:* Spray drying CFD modelling; Stochastic particle-wall collision model; Counter-current spray dryer kinetics

\* Corresponding author. Tel.: +44-0113-3432431.  
E-mail address: [t.mahmud@leeds.ac.uk](mailto:t.mahmud@leeds.ac.uk)

## 1. Introduction

Spray drying is one of the oldest methods used for the manufacture of particulate products in the food, chemical and pharmaceutical industries, and in the household and personal care products. It involves drying of droplets of a solution or slurry into particles by a hot gas. Thus converting a pumpable feed into dried powder in a single, continuous unit operation. The spray drying process involves multiphase flow with heat, mass and momentum transfer between the three-dimensional, complex, swirling, drying gas flow (continuous phase) and the discrete phase comprising polydispersed droplets/particles. Additionally, there is interaction between the droplets/particles, resulting in coalescence, agglomeration and breakage, as well as droplets/particle and wall interaction resulting in wall deposition, re-entrainment of deposited material, and breakage of particles. The aim of spray drying process is to produce dried powder of required characteristics (size distribution, moisture content, density, flowability etc.). Operating and design parameters can be varied to determine the optimum conditions for the required product attributes. This is carried out mainly by expensive and time consuming experimental investigations [1-3]. The modeling of spray drying towers can reduce the time and costs associated with the determination of optimized design and operating parameters. The complexity of gas flow patterns and interacting transport processes in spray drying towers poses challenges in the modeling of spray drying towers. The trajectories and hence the residence times of the droplets/particles are dependent on the gas flow patterns, therefore it is important to have a reliable prediction of gas flow profiles.

Computational Fluid Dynamics (CFD) is considered as the preferred choice of modeling spray drying towers. A number of studies have been published in the recent decades utilizing CFD for modeling spray drying towers. Most of these studies are focused on co-current spray drying towers, in which the droplets and drying gas are introduced from the top of the tower and the dried powder and the exhaust gas exit from the bottom of the tower. These towers are suitable for drying of heat sensitive products in food and pharmaceutical industries. Spray drying in counter-current towers is a poorly understood process as less attention has been given on the experimental study and modeling of these towers [5]. In the counter-current towers, the droplets are introduced from the top while the drying gas enters from the bottom using tangential-entry inlets that impart swirl to the gas flow. These towers are more thermally efficient compared to co-current towers and are used in the manufacture of thermally stable products like detergents and ceramics. The counter-current towers are typically tall-form (height to diameter ratio greater than 3). The droplets/particles in these towers exhibit frequent collision with the wall due to small diameter and the presence of swirling gas flow. In the earlier CFD studies reported on the modeling of counter-current spray drying towers [4, 6-8], the modeling of particle-wall interaction was ignored. The particle wall collision can result in wall deposition as well as dispersion of particles in the tower, thus directly influencing the residence times of particles, overall heat and mass transfer and the attributes of spray dried powder. The importance of modeling the particle-wall interaction was highlighted by Ali *et al.* [9] by allowing the restitution coefficient to vary with the moisture content. This significantly influenced the post-wall collision trajectories of the particles, residence times and the overall heat and mass transfer.

This study is focused on the CFD modeling of a pilot-plant counter-current spray drying tower used for detergent powder manufacture operated at P&G technical centres in Newcastle, UK. The gas (continuous phase) and droplets/particles (discrete phase) flow is considered to be steady state, three-dimensional, with the gas turbulence modeled using the Reynolds stress turbulence (RST) model. The model considers heat, mass and momentum transfer between the two phases coupled using Eulerian-Lagrangian approach. The droplet drying kinetics is modeled using a semi-empirical droplet drying model [10]. The work of Ali *et al.* [9] in modeling of the particle-wall interaction is extended by considering the restitution coefficient for particle-wall interaction a function of surface roughness in addition to the particle moisture content by developing a rough-wall collision model based on a stochastic approach. The commercial CFD software package Fluent v. 12 [18] is used for this purpose. The predicted dried powder moisture content, dried powder and exhaust gas temperatures are compared with data collected from the pilot-plant spray drying tower.

## Nomenclature

$T_{dep}, T_{amb}$	deposits surface temperature (K), ambient temperature (K)
$U$	overall heat transfer coefficient ( $W/m^2K$ )
$\dot{q}$	heat flux ( $W/m^2$ )
$C_{r,n}, C_{r,t}$	normal restitution coefficient, tangential restitution coefficient
$w_l$	moisture fraction
$\theta_{wp}$	angle between the rough wall surface and the impacting particle
$\Delta\theta$	standard deviation
$\theta_w$	surface roughness inclination angle (degree)
$\xi, \xi'$	Gaussian distributed random number, uniformly distributed random number
$l_s$	distance between the peaks of two successive roughness heights (m)
$k_s$	roughness height (m)
$\theta_{pi}$	particle inclination angle with the horizontal plane (degree)
$\theta_{pr}$	particle rebound angle with the horizontal plane (degree)
$d_p$	particle diameter
$h_1, h_2$	height at first particle-wall impact (m), height at second particle-wall impact (m)
$u_{pr,2}$	particle radial velocity component after first impact (m/s)
$u_{pz,2}$	particle axial velocity component after first impact (m/s)
$r, z$	radial coordinate, axial coordinate

## 2. Detergent slurry spray drying process

The detergent slurry prepared in a crutcher is a pumped to a hollow-cone pressure swirl nozzle atomizer using a series of low pressure and high pressure pumps. The pressure at the inlet of the atomizer is typically maintained at 60 to 70 barg. The drying gas is heated using a direct fired furnace typically in a temperature range of 250 to 300 °C. The temperature of the hot gas is measured at the outlet duct of the furnace. The hot gas is a mixture of drying gas and methane combustion products ( $CO_2$  and  $H_2O$ ), it is fed to the spray tower using a number of tangential-entry inlets near the tower bottom. The swirling hot gas flow inside the tower comes in contact with droplets/particles in a counter-current manner. The exhaust gas leaves from the tower top while the dried particles fall onto a belt conveyor, where its temperature is measured using an infrared probe, which is then air lifted and stored in a bin for sample collection. Several tests are carried out to assess the quality of the dried detergent powder including size distribution measurement, bulk density and measurement of moisture content. The exhaust gas contains entrained fine particles which are separated from the exhaust gas using a cyclone separator, the gas is then released to the atmosphere. The fine particles are either fed to the spray drier or recycled back to the slurry preparation unit. Figure 1 is a flow diagram of the spray drying process.

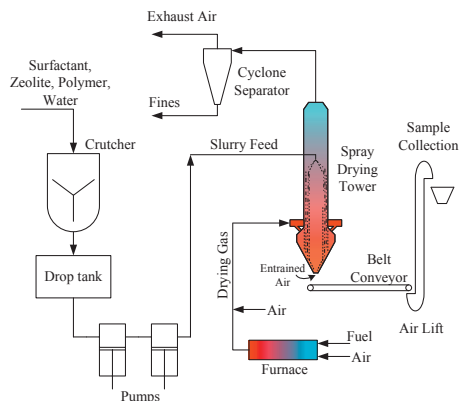


Figure 1: Process flow diagram of detergent slurry spray drying.

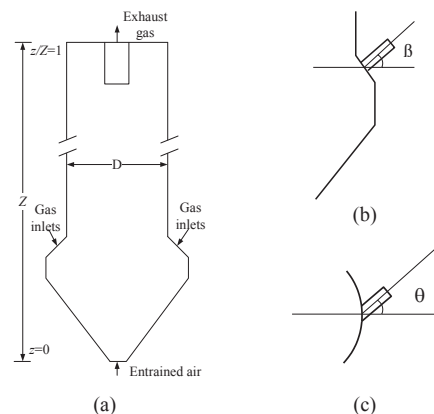


Figure 2: Schematic of the spray tower.

The counter-current spray drying tower studied is a pilot-plant tower with a height to diameter ratio greater than 3 and is depicted in Figure 2 (a). The actual dimensions of the tower are normalized with respect to the total tower height due to confidentiality reasons. The hot gas enters in the conical region of the tower via a number of inlets which are angled downwards and at an angle to the radius (Fig. 2 (b) and (c)). The latter gives a tangential velocity component to the hot gas and consequently causes a swirl to the gas flow.

### 3. CFD modeling of spray drying process

The continuous phase comprises hot gas and is modeled using the time averaged form of the continuity and Navier-Stokes equations [22]. The flow of hot gas inside the spray drying tower is a swirling flow. The turbulence is modeled using the Reynolds stress turbulence model. The selection of this model is based on an earlier investigation by Bayly *et al.* [11] carried out for modeling swirling air flow in a laboratory scale counter-current spray drying tower and its validation with measured data. The modeling of gas flow near the wall is carried out using the standard wall functions modified for surface roughness [12]. The transport of species and enthalpy through the continuous phase is modelled using the Reynolds-averaged scalar transport equations [22].

The heat loss due to conduction from the insulated tower wall with the inside of the wall containing a layer of deposits is carried out. The heat flux through the tower wall is given by the following equation:

$$\dot{q} = U(T_{dep} - T_{amb}) \quad (1)$$

where  $T_{dep}$  is the deposit surface temperature. In the evaluation of the overall heat transfer coefficient ( $U$ ), the thermal resistance due to the deposits layer, wall, insulation and the outside convective film is considered.

The discrete phase is modelled using the Lagrangian approach. The trajectories of the droplets/particles are calculated by solving the equation of motion by considering the drag, the buoyancy and the gravitational forces. The drag coefficient used for computing drag force on the particles is calculated using the correlation proposed by Morsi and Alexander [13], applicable to smooth spherical particles. For the droplet drying kinetics, a three-stage semi-empirical droplet drying model [10] developed in house by P&G is used to model heat and mass transfer between the two phases. The description of the droplet drying model along with the drying model equations are given elsewhere [14]. The droplet drying model is incorporated in Fluent using user-defined functions.

### 4. Modeling of particle-wall interaction

The equation given by Ali *et al.* [9] for the restitution coefficient considers the variation as a linear function of moisture content with a limiting value of 0 for the initial droplets and a maximum value of 0.4 for the dried detergent particles. It is used for computing the tangential restitution coefficient ( $C_{r,t}$ ).  $C_{r,t}$  computes the post wall collision particle velocity parallel to the wall, which directly influences the residence time of particles. The normal restitution coefficient ( $C_{r,n}$ ) is responsible for calculating the particle velocity normal to the wall, thus it influences the dispersion of the particles over the tower cross-section. This is specified as a function of particle-wall impact angle. The correlation for  $C_{r,n}$  is based on the work by Hassal [15] in which the variation in the restitution coefficient was studied by impacting the dried detergent particles on a smooth surface at various impact angles. The tangential and normal restitution coefficients are given by equations (2) and (3) respectively.

$$C_{r,t} = -0.4 \left( \frac{w_l}{w_{l,o}} \right) + 0.4 \quad (2)$$

$$C_{r,n} = -0.0033 \theta_{wp} + 0.45 \quad (3)$$

The particles post-wall collision velocities tangent and normal to the wall are then calculated using equations (4) and (5) respectively.

$$v_{2,t} = C_{r,t} v_{1,t} \tag{4}$$

$$v_{2,n} = C_{r,n} v_{1,n} \tag{5}$$

where  $v_{2,t}$  and  $v_{2,n}$  are the post-wall collision velocity components tangent and normal to the rough wall respectively.

A stochastic model for the collision between the particle and the wall has been developed that generates the virtual rough wall surface roughness inclination angle at the particle-wall impact location. The angle between the virtual rough wall surface and the impacting particle ( $\theta_{wp}$ ) is then used in equation (3) to calculate the normal restitution coefficient. The inclination angle of the virtual rough wall surface is determined by a Gaussian/normal distribution of surface roughness inclination angles with a mean value of zero and a standard deviation of 3.0. The range of wall surface roughness angles are considered from  $-90^\circ$  to  $90^\circ$ . Additionally the probability of multiple particle rebound is evaluated and its effect on the particle trajectory is also calculated. The impacting particles are assumed to be smooth spherical and the possibility of deposition of particles on the wall is ignored. Figure 3 depicts different particle-rough wall collision scenarios.

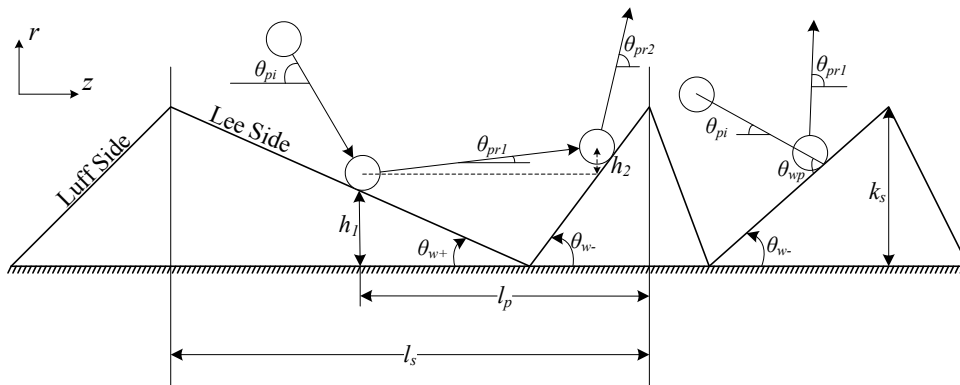


Figure 3: Particle-rough wall collision scenarios.

The angle of inclination of the virtual rough wall surface is sampled from a random variable with a Gaussian distribution as mentioned above. Same approach was used by Sommerfeld and Huber [16] in generating a rough surface inclination angle. It is given by the following equation:

$$\theta_w = \Delta\theta \frac{\xi}{3} \tag{6}$$

In the above equation,  $\xi$  is a random number obtained from a Gaussian/normal distribution, and  $\Delta\theta$  is the standard deviation of roughness angles, which is taken to be  $90^\circ$ . Thus the generated surface inclination angle for the virtual rough wall ranges from  $-90$  to  $90^\circ$ , according to Gaussian/normal distribution.

If the sampled surface inclination angle is negative, then the particle will hit the luff side of the roughness, otherwise it will hit the lee side. But due to the shadow effect on the lee side, the impacting particle can only hit this side when the sampled surface roughness inclination angle ( $\theta_{w+}$ ) is less than the particle inclination angle  $\theta_{pi}$ . If  $\theta_{w+} > \theta_{pi}$ , a new surface inclination angle is sampled, the expressions are given by equation (7):

$$\theta_w = \begin{cases} \theta_{w+} & \text{if } (\theta_w > 0) \text{ and } (\theta_w < \theta_{pi}) \\ \theta_{w-} & \text{if } (\theta_w < 0) \end{cases} \tag{7}$$

If the particle is hitting the lee side of the surface roughness, then the surface roughness angle of the luff side is determined and vice versa in order to evaluate the possibility of multiple particle rebound. The length between the peaks of two successive roughness inclinations ( $l_s$ ) is then calculated using the following equation:

$$l_s = k_s \left( \frac{1}{\tan(|\theta_{w+}|)} + \frac{1}{\tan(|\theta_{w-}|)} \right) \quad (8)$$

In the following scenarios, only a single collision will take place between the particle and the wall:

- If the particle hits the luff side and the particle-wall impact angle ( $\theta_{wp}$ ) is less than  $90^\circ$ .
- If the particle hits the lee side and the particle rebound angle ( $\theta_{prl}$ ) is greater than or equal to the roughness inclination angle of the luff side ( $|\theta_{w-}|$ ).
- If the diameter of the particle is greater than  $l_s$ .

The particle post wall collision velocity components are determined by the tangential and normal restitution coefficients, equation (2) and (3), respectively. To evaluate whether multiple particle rebound occurs, the post collision angle ( $\theta_{prl}$ ) is required, which is calculated using the following equation:

$$\theta_{prl} = \tan^{-1} \left( \frac{u_{pr,2}}{u_{pz,2}} \right) \quad (9)$$

The height of the particle-wall impact location is determined by stochastic approach, using the following equation:

$$h_1 = k_s \zeta' \quad (10)$$

where  $\zeta'$  is a uniformly distributed random number in a range of 0 to 1.

The height traversed by the rebound particle at a distance  $l_p$  from the first impact location is calculated using the following equation:

$$h_2 = \left( \frac{h_1}{\tan(|\theta_{w+}|)} + \frac{k_s}{\tan(|\theta_{w-}|)} - d_p \right) \times \tan(\theta_{prl}) \quad (11)$$

If the sum of  $h_1$  and  $h_2$  is less than the roughness height ( $k_s$ ), then the particle will rebound with the wall again. The post rebound velocity of the particle is then again calculated using the tangential and normal restitution coefficients given by equation (2) and (3) respectively. The particle-rough wall collision has been applied to the modeling of a pilot-plant counter-current spray drying process to predict post particle-wall collision trajectories. The model is incorporated in Fluent using user-defined functions. The value of roughness height ( $k_s$ ) is specified to be 2 mm.

## 5. Model application

Two CFD Cases are presented in this paper. In the first case (referred to as Case 1), both the tangential and normal components of restitution coefficients are considered as a linear function of moisture content, given by equation (2). In the second case (Case 2), the proposed rough-wall collision model is applied to calculate the normal restitution coefficient (given by equation 3) while the tangential restitution coefficient is calculated using equation (2). Due to the absence of atomized slurry droplet size distribution at the nozzle, the measured dried powder size distribution is specified. It ranges from 100  $\mu\text{m}$  to 2300  $\mu\text{m}$  and is fitted using Rosin-Rammler distribution using a size constant of 750  $\mu\text{m}$  and a distribution parameter of 1.35. The operating conditions obtained from a pilot-plant drying tower are used for both CFD simulation cases and are listed in Table 1.

Table 1. Input specifications for CFD simulation cases.

Droplet Properties			Gas Properties		
Slurry inlet temperature	358	K	Hot gas temperature	563	K
Slurry mass flux	0.21	kg/m <sup>2</sup> s	Hot gas mass flux	0.92	kg/m <sup>2</sup> s
Specific heat of dried particles	1500	J/kgK	Entrained air mass flux	0.046	kg/m <sup>2</sup> s
Specific heat of solvent	4180	J/kgK	Entrained air/ambient temperature	293	K
Specific heat of vapors	1900	J/kgK	Column Wall		
Density of slurry	1200	kg/m <sup>3</sup>	Wall thickness	0.006	m
Latent heat of vaporization	2.26×10 <sup>6</sup>	J/kg	Wall thermal conductivity	18.8	W/mK
Moisture diffusivity	3.0×10 <sup>-11</sup>	m <sup>2</sup> /s	Insulation thickness	0.105	m
Vapors diffusivity	2.6×10 <sup>-5</sup>	m <sup>2</sup> /s	Insulation conductivity	0.04	W/mK
Droplet initial velocity	74.5	m/s	Deposits thickness	0.002	m
Spray nozzle dimensionless height (z/Z)	0.67		Deposits conductivity	1.3	W/mK

The tower geometry and meshing was carried out using meshing software [17]. The selected mesh comprised  $1.3 \times 10^6$  tetrahedral computational cells. The selected mesh size was based on a comparison of single phase isothermal velocity profiles using three different mesh sizes and the selected mesh was the optimum in terms of computational time and precision. The conservation equations for the continuous and discrete phases are solved using the commercial CFD software Fluent v. 12 [18], which is based on the finite volume method.

For the inlet boundary conditions, velocity magnitude is specified at the inlet faces of the hot gas and the cold entrained air. For the outlet boundary condition, pressure outlet with a value of -300 Pa is specified. For the turbulence boundary conditions, a turbulent intensity of 5% at the inlet face along with the hydraulic diameter of the inlet is specified. The Reynolds stresses at the boundary faces are calculated from the assumption of isotropy of turbulence. To take into account for wall roughness due to deposits, a roughness height of 2 mm and a roughness constant of 1.0 are specified in the log-law of the wall modified for surface roughness [12]. The gas phase density is considered a function of composition and is calculated using the ideal gas law while the viscosity is allowed to vary with temperature. For the turbulent diffusion flux in the energy equation, a value of 0.85 is used.

For solving the gas and the discrete phase, steady state approximation is used. For pressure-velocity coupling PISO scheme [19] is used and for pressure interpolation, PRESTO! scheme [20] is used. The convective terms are discretized using the second order upwind discretization scheme. The convergence criteria for the continuity, momentum, species and Reynolds stresses were specified as  $1 \times 10^{-4}$ , for the energy equation, it was  $1 \times 10^{-6}$ . The polydispersed droplets/particles are represented using 23 discrete sizes and a total of 3700 parcels. The effect of gas turbulence on the droplet/particle dispersion is taken into account using the discrete random walk model [18]. Particle-particle interactions and hence coalescence and agglomeration is ignored due to large computational requirements.

The multiphase flow simulation was initialized from a converged gas flow fields by injecting the droplets in a hollow cone spray pattern with a spray cone half angle of  $20^\circ$ . The residuals of continuity, momentum and turbulence quantities could not converge to the required tolerance limits; therefore the exhaust gas temperature (which is an indicator of the overall heat and mass transfer between the discrete phase and the gas phase) was monitored. The simulation runs were stopped once a steady exhaust gas temperature was obtained.

## 6. Results and discussion

Figure 4 (a) and (b) is a plot of selected number of predicted trajectories of the droplets/particles in the cylindrical region of the tower, colored by diameter. Smaller particle sizes (up to 200  $\mu\text{m}$ ) get entrained by the gas while the larger sizes exit from the tower bottom. Smaller sizes at the tower bottom (up to 300  $\mu\text{m}$ ) in both cases start to swirl as they flow downward due to the swirling gas flow. From a comparison of predicted particle trajectories in both cases it is observed that the particles hitting the wall in Case 1 (Figure (4a)), start to flow downwards and remain

close to the wall due to the use of  $C_r$  as a function of moisture content only. But in Case 2 (Figure (4b)), the particles get rebound from the wall at different angles since the normal component of restitution coefficient ( $C_{r,n}$ ) is calculated using the rough-wall collision model. Hence in Case 2, the particles get dispersed over the cross-section after collision with the wall. Figure (4c) and (4d) depict contours of velocity magnitude for case 1 and 2 respectively. The gas flow in the bottom cylindrical region ( $z/Z = 0.15$  to  $0.5$ ) is symmetrical while above the spray nozzle it is asymmetrical in both cases. At  $z/Z = 0.15$  to  $0.5$ , the gas velocity magnitude is high in the annular region and lower in the central region of the tower, due to the swirling gas flow. A high velocity jet is observed at the spray location with entrained gas flow in Figure (4e) for Case 1 and Figure (4f) for Case 2. The gas flow is in the upward direction close to the wall while it is flowing downwards inside the spray due to momentum exerted by the sprayed droplets onto the gas. The flow is relatively more evenly distributed around the spray in Case 1 (Figure 4e), whereas in Figure (4f) it is asymmetrical. Uneven distribution of the gas flow around the spray is undesirable as it can lead to impingement of the droplets onto the wall causing excessive wall deposition.

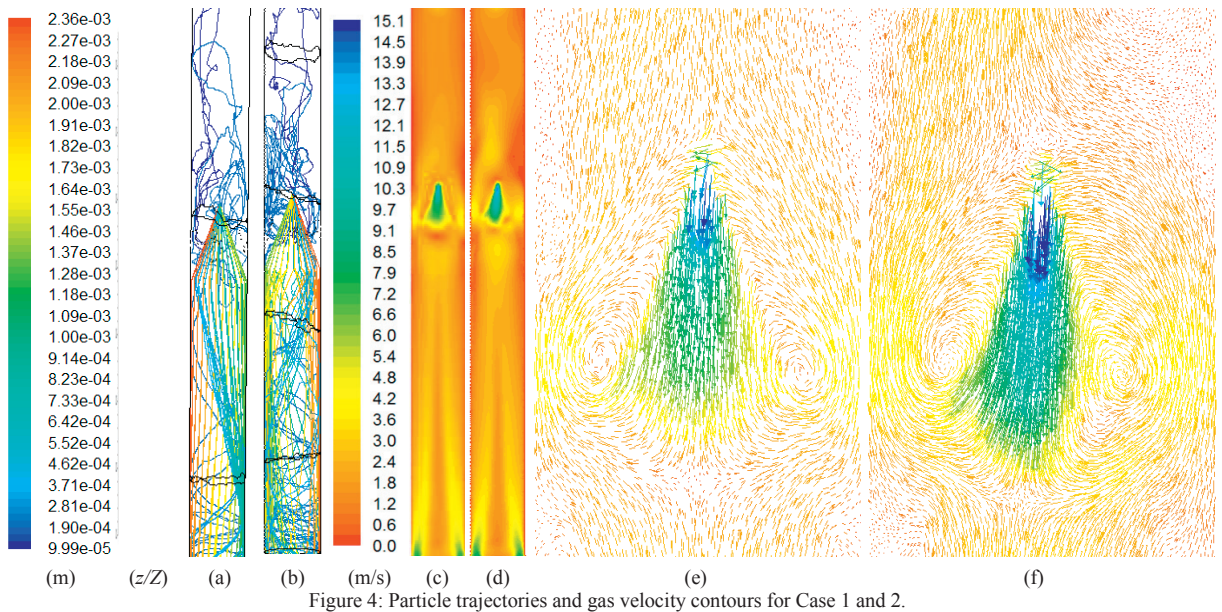


Figure 4: Particle trajectories and gas velocity contours for Case 1 and 2.

Figure 5 (a) and (b) are plots of the discrete phase concentrations along the dimensionless tower radius. The discrete phase concentration represents the mass flow of the discrete phase passing through a computational domain per unit cell volume and time. A higher concentration is observed near the wall and a lower concentration towards the centerline. At  $z/Z = 0.56$  (below the nozzle), a significant difference in the discrete phase concentration between the two cases is observed. In Case 2, the concentration is relatively higher near the wall as well as along the radius hence the particles are more dispersed when they rebound with a rough wall, in contrast to Case 1, in which the particles are concentrated towards the wall only. At  $z/Z=0.29$ , both Cases give similar concentrations of the discrete phase because as the particles flow further downwards, the centrifugal force due to swirling flow causes the particles to move close to the wall. The particles exit residence times are depicted in Figure 5(c). Smaller particles in both cases have a significantly larger residence time as they have less momentum and therefore exhibit greater influence of the drag force acting opposite to the particle flow. The residence times of particles in both cases are very similar, primarily because both cases consider  $C_{r,t}$  a linear function of moisture, which is used for calculating post-collision velocity parallel to the wall.

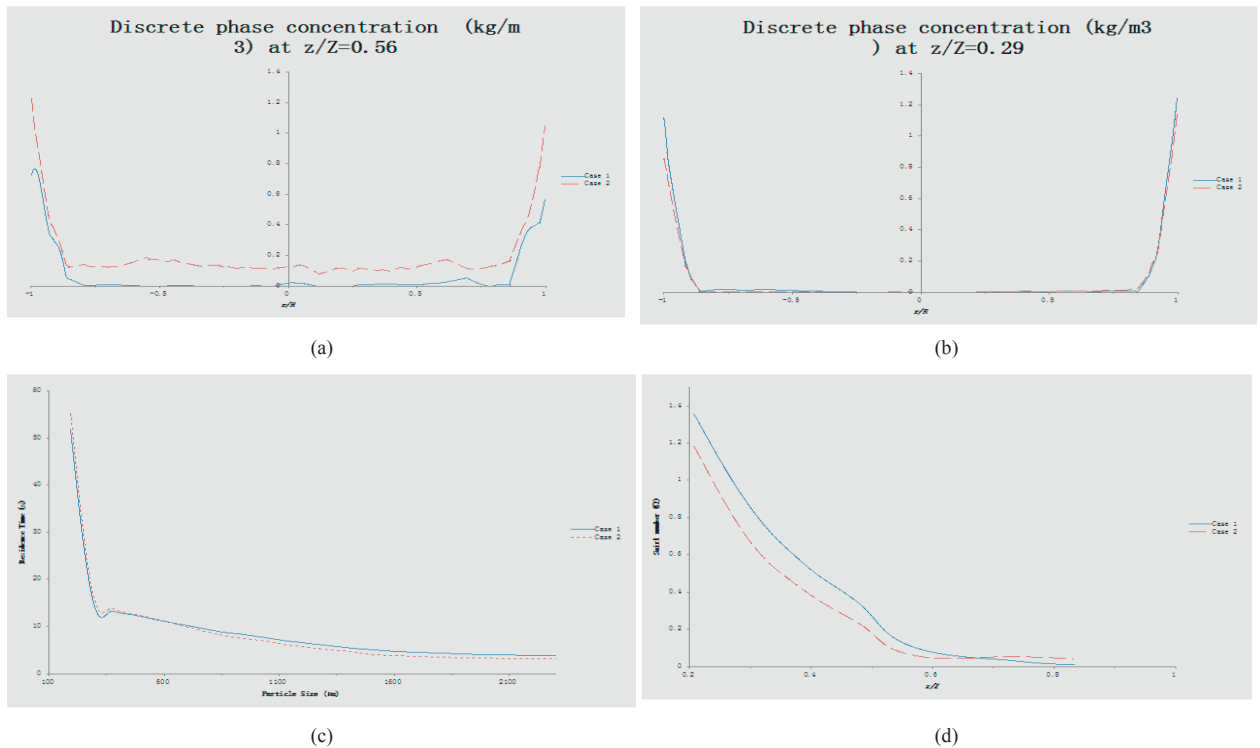


Figure 5: Discrete phase concentration, particles residence times and swirl number for Case 1 and 2.

Figure 5 (d) depicts swirl number along the dimensionless tower height. The swirl number characterizes the strength of a swirling flow and is defined as the ratio between the angular and axial momentum flux [21]. The swirl number is higher in the bottom cylindrical region and decreases as the gas flows upwards as the gas loses its angular momentum due to exchange with particles, the swirl decay is also due to the wall surface roughness. From a comparison of swirl number in both cases, it is observed that below the spray nozzle ( $z/Z = 0.67$ ) the swirl number is lower in Case 2 compared to Case 1, however above  $z/Z=0.6$ , a greater decay in swirl is observed in Case 1 and the swirl is zero above  $z/Z=0.8$ , while in Case 2, the swirl decay is slightly slower along the height above  $z/Z=0.67$ .

A comparison of CFD simulation cases with the measured data is given in Table 2. It is observed that Case 2 gives a closer agreement with measured moisture content and outlet gas temperature compared to Case 1 which predicts a greater moisture content and a higher outlet gas temperature. This is because in Case 2 the particles after rebound with the wall are more dispersed over the tower cross-section and the gas temperature is relatively higher in the central region of the tower compared to the near-wall region and hence greater heat and mass transfer takes place in Case 2. The particles average outlet temperature is significantly greater in both cases since the measurement of powder temperature is made at the belt conveyor a few meters away from the bottom exit location, the particles are expected to cool down as they come in contact with surrounding air at the belt, which is not taken into account in the CFD simulations. The heat loss in both CFD Cases is similar, but significantly lower than that based on the measured temperatures, mainly because the temperature measurement is taken at the hot gas supply duct and includes the heat loss that takes place from the duct to the tower gas inlets.

Table 2. CFD simulation cases comparison with measurements.

Parameter	Case 1	Case 2	Measured
Particle weighted average moisture content, %	4.75	3.09	1.8
Particle weighted average temperature, K	456.19	467.7	356
Outlet gas temperature, K	381.4	377.7	367
Heat loss, kW	5.4	5.6	62.1

## 7. Conclusions

Multiphase CFD modeling of a pilot-plant counter-current spray drying tower was carried out considering heat, mass and momentum transfer between the droplets/particles and the drying gas. A particle rough-wall collision model was developed and applied on spray drying process to study the importance of particles dispersion due to collision with a rough wall and on the particle trajectories and the overall heat and mass transfer. It was found that the particle-wall interaction was one of the critical factors that significantly influenced the predicted average dried powder characteristics. A comparison was made with the measured dried powder average characteristics and exhaust gas temperature and the case incorporating the rough-wall collision model gave a closer prediction with the measurements.

## Acknowledgements

Financial support by Procter and Gamble, Newcastle Innovation Centre and from IPSE, University of Leeds for the first author is gratefully acknowledged. The authors would like to thank Mr. Zayeed Alam, Procter and Gamble for his support and encouragement.

## References

- [1] K. Masters, *Spray Drying: An Introduction to Principles, Operational Practice and Applications*, Leonard Hill Books, London, 1972.
- [2] E.R. Bahu, *Spray Drying – Maturity or Opportunities? Drying '92*, part - A, (1992) 74-91.
- [3] T.A.G. Langrish, D.F. Fletcher, *Prospects for the Modelling and Design of Spray Dryers in the 21st Century*, *Drying Technology*, 21 (2003) 197-215.
- [4] D.M. Livesley, D.E. Oakley, R.F. Gillespie, C.K. Ranpuria, T. Taylor, W. Wood, M.L. Yeoman, *Development and validation of a computational model for spray-gas mixing in spray dryers*. *Drying '92*, Ed. Mujumdar, A. S., pp. 407-416, New York: Hemisphere Publishing Corp, 1992.
- [5] I. Zbicinski, M. Piatkowski, *Continuous and discrete phase behavior in countercurrent spray drying process*, *Drying Technology*, 27 (2009) 1353-1362.
- [6] C.T. Crowe, *Droplet-gas interaction in counter-current spray dryers*, *Drying Technology*, 1 (1983) 35-56.
- [7] I. Zbicinski, R. Zietara, *CFD model of counter-current spray drying process*, in: *Proceedings of the 14th International Drying Symposium*, 2004, Sao Paulo, 22-25 August, vol. A, (2004) 169-176.
- [8] P. Wawrzyniak, M. Podyma, I. Zbicinski, Z. Bartczak, A. Polanczyk, J. Rabaeva, *Model of heat and mass transfer in an industrial counter-current spray-drying tower*, *Drying Technology*, 30 (2012) 1274-1282.
- [9] M. Ali, T. Mahmud, P.J. Heggs, M. Ghadiri, V. Francia, H. Ahmadian, L. Martindejuan, D. Djurdjevic, A. Bayly, *CFD modelling of a counter-current spray drying tower*, in: *8th International Conference on Multiphase Flow ICMF*, 2013, Jeju, South Korea, 26-31 May 2013.
- [10] J.P. Hecht, *Personal Communication*, P&G Technical Centres, UK, 2012.
- [11] A.E. Bayly, P. Jukes, M. Groombridge, C. McNally, *Airflow patterns in a counter-current spray drying tower – simulation and measurement*, in: *Proceedings of the 14th International Drying Symposium*, 2004, Sao Paulo, 22-25 August, vol. B, (2004) 775-781.
- [12] T. Cebeci, P. Bradshaw, *Momentum Transfer in Boundary Layers*, McGraw-Hill, London, 1977.
- [13] S.A. Morsi, A.J. Alexander, *An investigation of particle trajectories in two-phase flow systems*, *J. Fluid Mech.*, 55 (1972) 193-208.
- [14] M. Ali, T. Mahmud, P.J. Heggs, M. Ghadiri, D. Djurdjevic, H. Ahmadian, L.M. Juan, C. Amador, A. Bayly, *A one-dimensional plug-flow model of a counter-current spray drying tower*. *Chem. Eng. Res. Des.*, In Press, Available Online August 2013, <http://dx.doi.org/10.1016/j.cherd.2013.08.010>
- [15] G.J. Hassal, *Wall build-up in spray dryers*, Ph.D. Thesis, University of Birmingham, UK, 2011.
- [16] M. Sommerfeld, N. Huber, *Experimental analysis and modelling of particle-wall collisions*, *Int. J. Multiphas. Flow*, 25 (1999) 1457-1489.
- [17] *Gambit*, version 2.4, <http://www.ansys.com>
- [18] *Fluent User's guide*. Ansys Inc, 2009.

- [19] R.I. Issa, Solution of the implicitly discretised fluid flow equations by operator splitting, *J. Comp. Phy.*, 62 (1985) 40-65.
- [20] S.V. Patankar, *Numerical Heat Transfer and Fluid Flow*. Hemisphere, Washington, 1980.
- [21] K.S. Yajnik, M.V. Subbaiah, Experiments on swirling turbulent flows. *J. Fluid Mech.*, 60 (1973) 665-687.
- [22] H.K. Versteeg, W. Malalasekera, *An Introduction to Computational Fluid Dynamics*, Longman Scientific and Technical, Harlow, 1995.